

Article

Edible Films Based on Ovine Second Cheese Whey with Oregano Essential Oil

Arona Pires ^{1,2,3}, Angel Cobos ¹ , Carlos Pereira ^{2,3}  and Olga Díaz ^{1,*} 

¹ Área de Tecnología de Alimentos, Departamento de Química Analítica, Nutrición y Bromatología, Facultad de Ciencias, Campus Terra, Universidade de Santiago de Compostela, 27002 Lugo, Spain; arona@esac.pt (A.P.); angel.cobos@usc.es (A.C.)

² School of Agriculture, Bencanta, Polytechnic University of Coimbra, 3045-601 Coimbra, Portugal; cpereira@esac.pt

³ Centro de Estudos dos Recursos Naturais, Ambiente e Sociedade—CERNAS, 3045-601 Coimbra, Portugal

* Correspondence: olga.diaz.rubio@usc.es

Abstract: The aim of this study was to produce edible films using ovine second cheese whey (SCW) powder, alone or combined with whey protein isolate (WPI). SCW is a by-product obtained in the manufacture of ovine whey cheeses. In this instance, it was dehydrated after increasing the protein concentration by ultrafiltration/diafiltration. Furthermore, the effects of the addition of oregano (*Origanum compactum*) essential oil (EO) in two proportions to the films produced with a mixture of SCW powder and WPI were studied. The water vapor permeability, solubility, color, opacity, antioxidant activity, and the mechanical properties of the films were determined. In addition, we determined the films' structure, by FTIR; thermal stability, by TGA; and microstructure and crystallinity, by XRD. SCW combined with WPI can be used to prepare edible films, but their properties were found to be affected depending on the proportion of each product. The substitution of WPI by SCW caused decreases in water solubility (from 81.44 to 66.49% D.M.), modified the color and decreased tensile strength (from 1.57 to 0.17 MPa), and decreased the elongation at break (from 52.17 to 3.57%), the puncture strength (from 2.40 to 0.20 MPa) and the deformation (from 18.92 to 0.93%) of the films. EO addition to the SCW–WPI films increased the antioxidant activity of the films (from 0.97 to 2.19 mg DPPH/g). It also modified other characteristics of the films such as the water solubility and the tensile strength. Both SCW and EO incorporations influenced the secondary structure of proteins and the thermal stability, microstructure and crystallinity of the films.

Keywords: edible packaging; sheep cheese whey; essential oils; antioxidant; mechanical properties; FTIR; TGA; microstructure; XRD



Academic Editor: Nikolay D. Menkov

Received: 10 April 2025

Revised: 4 May 2025

Accepted: 7 May 2025

Published: 9 May 2025

Citation: Pires, A.; Cobos, A.; Pereira, C.; Díaz, O. Edible Films Based on Ovine Second Cheese Whey with Oregano Essential Oil. *Appl. Sci.* **2025**, *15*, 5325. <https://doi.org/10.3390/app15105325>

Copyright: © 2025 by the authors. Licensee MDPI, Basel, Switzerland. This article is an open access article distributed under the terms and conditions of the Creative Commons Attribution (CC BY) license (<https://creativecommons.org/licenses/by/4.0/>).

1. Introduction

The preservation of food products, extending their shelf life, and the sustainability of companies are some of the most important challenges that industries face. Food that is not stored safely and hygienically can cause serious negative health effects. The most used packaging is plastic, followed by glass, metal and paper [1]. Due to its durability, design flexibility, lightness and low price, plastic packaging has become advantageous over other raw materials for packaging food products [2]. Plastic films derived from petroleum are widely utilized due to their ease of production, cost-effectiveness, and satisfactory mechanical properties. These films aid in preserving the quality of food products by restricting the permeation of water vapor, oxygen, carbon dioxide, and aromatic

compounds. However, conventional packaging materials are associated with challenges related to recycling, inability to degrade after disposal, detrimental environmental and wildlife impacts, and utilization of finite fossil fuel reserves. Additionally, the presence of microplastics and the potential migration of harmful additives from plastic packaging into food pose significant health risks and concerns [2]. Regulation 2025/40 of the European Union restricts the utilization of certain single-use plastics and minimizes the weight and volume of packaging, the waste produced and the inclusion of some additives in the materials [3].

The food sector is one of the biggest contributors to global greenhouse gas emissions (approximately 26%) and, consequently, food waste contributes to the negative impact of climate change, since much of the food produced is not consumed. Therefore, to minimize these negative impacts, new packaging must be able to guarantee food quality and safety, as well as increase the shelf life of food and be edible or easily recyclable [1]. These reasons explain why we continue to develop sustainable and fully biodegradable packaging materials, including edible films and coatings, providing a long shelf life for food and thus promoting the safe integration of packaging [1]. Thus, packaging materials obtained from biopolymers such as proteins, polysaccharides and lipids are a good alternative to petroleum-derived materials (synthetic materials) since they are obtained from renewable sources or biodegradable industrial by-products and do not adversely affect the environment [2,4].

Protein-based films are a sustainable and efficient alternative for food packaging [5]. These films are produced from proteins extracted from various sources, such as cheese whey, wheat and corn [6–8]. They have advantages in terms of biodegradability, are edible, and have good barrier properties that help preserve food against moisture, oxygen and light [2].

Whey protein-based edible films have become an interesting innovation in the food industry as a food packaging material, due to their sustainability and nutritional characteristics. The whey is a by-product of cheese production, and the protein is concentrated mainly by membrane processes that obtain whey protein concentrate (WPC) and whey protein isolate (WPI). These products contain valuable essential amino acids and are useful to produce edible films and coatings [2,9–11]. These edible films can reduce food waste and act as barriers against oxygen and aromatic compounds with good mechanical properties [9]. It has also been indicated that WPI films in substitution of fossil polymers could be useful to reduce environmental contamination due to the reduction of electricity consumption [10]. These studies have been done with protein films obtained from bovine whey. We have not found works related to the application of ovine whey in edible films.

The second cheese whey (SCW) is a by-product generated in the whey cheese production. Whey cheese is obtained by heating whey at 85–90 °C for 20–30 min to facilitate the denaturation of whey proteins, which results in their aggregation; SCW is the liquid remaining after protein aggregates recovery [9]. Although a high proportion of this product is discarded without treatment, it contains proteins, mainly in a denatured state, that are beneficial to human health, can be used in the manufacture of foods such as fermented drinks or dressings, and can also be useful in the production of edible films and coatings with excellent nutritional and functional properties [9]. However, the use of SCW in the production of edible coatings and films has been mostly ignored, and its potential as a sustainable packaging material has remained unstudied.

To date, only one study has been found referring to the use of SCW as a material for the production of edible films [12]. Alfano et al. investigated the use of buffalo second cheese whey (SCW) to obtain films. They treated buffalo SCW with microfiltration and ultrafiltration and obtained two retentates of 100 kDa and 10 kDa. They obtained removable

and reusable film with a thickness of 100 μm only with the retentate of 10 kDa, using glycerol as plasticizer. The characteristics of the films are not described in this study [12]. There are no studies of films obtained with ovine SCW.

In one article of our research group, Pires et al. [13] used sheep SCW in a mixture with WPI with 8% (w/v) protein (in the proportion 2:1 SCW/WPI) and with glycerol as plasticizer in order to prepare cheese coatings with or without oregano or clary sage essential oils. To obtain SCW powder, ultrafiltration (10 kDa cutoff), diafiltration, reverse osmosis and lyophilization processes were used. Cheeses with SCW/WPI coatings had higher water activity, higher moisture content (due to prevent high evaporation), lower titratable acidity and lower chewiness, hardness and gumminess at the end of ripening than cheeses without coating or with commercial coating with natamycin. Additionally, it was concluded that coatings made with SCW and WPI can successfully replace commercial coatings [13].

The addition of essential oils, such as oregano essential oil, to films manufactured with WPC or WPI has been investigated due to their antimicrobial and antioxidant effects [14–17]. However, this incorporation has some effects on some of the properties, such as water permeability and the flexibility of the films [16–18].

The development of edible films with a mixture of SCW and WPI and the addition of essential oils could also be interesting for food packaging. However, their properties are different to those of the coatings and must be studied before application in the food industry because the proportion of SCW, WPI and essential oils can influence their efficiency.

One objective of this work was to develop edible films based on ovine SCW powders, alone or combined with different proportions of bovine WPI, and to compare the water vapor permeability, solubility, color, opacity, antioxidant activity, mechanical properties, structure (by FTIR), thermal stability (by TGA), microstructure and crystallinity (by XRD) of the films. The second aim was to study these properties in films obtained with ovine SCW and WPI incorporating oregano (*Origanum compactum*) essential oil (EO) in two different percentages.

2. Materials and Methods

2.1. Materials

Bovine whey protein isolate (NatWPI90, 90% w/w protein, 1.0% fat, 2.5% ash) was supplied by InLeit Ingredients S.L.U. (Curtis, Spain). Ovine second cheese whey powder (54.7% w/w protein, 14.3% fat, 7.9% ash) was obtained after ultrafiltration/diafiltration, pasteurization, reverse osmosis and freeze drying of SCW, as indicated by Pires et al. [13].

2.2. Films Preparation

Firstly, five different films were obtained with five different concentrations of WPI and SCW powders. WPI and SCW were weighed to obtain a final protein concentration of 8% (w/v) in the film-forming solution. The films were prepared in the following manner: The WPI was dissolved in distilled water using a magnetic stirrer at 20 $^{\circ}\text{C}$ for 30 min and glycerol (Panreac, Barcelona, Spain) was incorporated at a protein-to-plasticizer ratio of 1:1. The pH was then adjusted to 7.0 using 0.1 M NaOH. Thereafter, the WPI–plasticizer solution was heated to 90 $^{\circ}\text{C}$ for 15 min with constant stirring. This process was conducted in an electronic magnetic stirred hot plate (VELP Scientifica, Usmate, Italy) connected to a digital temperature controller (VTF Digital Thermoregulator, VELP Scientifica, Usmate, Italy) to ensure precise temperature regulation. Then, the solutions were cooled to room temperature and degassed under vacuum for 15 min. The films composed exclusively of SCW were prepared in a similar manner except that the heating step was omitted. In the films containing WPI + SCW (in three proportions of WPI:SCW, 2:1, 1:1, and 1:2), the SCW powder was incorporated into the WPI–plasticizer solution after the cooling

step. The mixture was then homogenized using an Ultra-Turrax (model T18 basic; IKA™, Staufen, Germany) for 3 min operating at 15,500 rpm. Finally, the pH of the solution was readjusted to a value of 7 using 0.1 M NaOH. Subsequently, degassing was conducted under vacuum for 15 min. Thereafter, all film-forming solutions (0.22 g cm^{-2}) were dispensed into Plexiglas Petri dishes (14 cm diameter) and were subjected to drying at $50 \text{ }^\circ\text{C}$ for 20 h within an air force cabinet. Before being peeled off, the dried films were transferred to a climate chamber (Ensayos Terlab S.L., Barcelona, Spain) and maintained at 45% relative humidity and $25 \text{ }^\circ\text{C}$ for 48 h. The peeled films were finally stored in a desiccator at 45% relative humidity and room temperature for additional testing. The experiments were conducted in triplicate.

Secondly, six different films were prepared with the addition of oregano (*Origanum compactum*) essential oil (Plena Natura, Amadora, Portugal). The films were prepared in the following way: the preparations of WPI–plasticizer solution, after heat treatment and cooling, were separated into six equal portions to prepare the films containing the three proportions of WPI:SCW (2:1, 1:1 and 1:2) and two different proportions of oregano essential oil (EO) (1 and 2% of the powder weight in solution). The EO and the SCW powder were added simultaneously to the previously prepared WPI–plasticizer solution and the mixtures were homogenized using an Ultra-Turrax homogenizer. The final pH was adjusted to 7 with 0.1 M NaOH, and the films were formed as indicated before. The experiments were performed in triplicate.

Summarizing, eleven different films were obtained.

1. WPI: films only with whey protein isolate.
2. WS 2:1: films of WPI–SCW mixture in a protein proportion of 2:1.
3. WS 1:1: films of WPI–SCW mixture in a protein proportion of 1:1.
4. WS 1:2: films of WPI–SCW mixture in a protein proportion 1:2.
5. SCW: films only with ovine second cheese whey.
6. WS 2:1O1: films of WPI–SCW mixture in protein proportion 2:1 with 1% EO.
7. WS 1:1O1: films of WPI–SCW mixture in protein proportion 1:1 with 1% EO.
8. WS 1:2O1: films of WPI–SCW mixture in protein proportion 1:2 with 1% EO.
9. WS 2:1O2: films of WPI–SCW mixture in protein proportion 2:1 with 2% EO.
10. WS 1:1O2: films of WPI–SCW mixture in protein proportion 1:1 with 2% EO.
11. WS 1:2O2: films of WPI–SCW mixture in protein proportion 1:2 with 2% EO.

2.3. Film Thickness

Film thickness was measured as per the method described by Cobos and Díaz [19] using a 0–25 mm electronic digital micrometer with 0.001 mm accuracy (Selecta, Barcelona, Spain) at 20 random points of three films.

2.4. Water Vapor Permeability

Water vapor permeability (WVP) was determined according to the ASTM E-96-93 method [20] with some modifications [19]. Measurements were conducted in triplicate. WVP was calculated using Equation (1):

$$\text{WVP} \left(\text{ng s}^{-1} \text{ m}^{-1} \text{ Pa}^{-1} \right) = \frac{w \times L}{A \times \Delta t \times \Delta P} \quad (1)$$

where w is the weight increase of the cell (ng) for time of permeation Δt (s); L is the thickness of the film (m); A is the film permeation area (m^2); and ΔP is the difference in water vapor pressure (Pa) through the film.

2.5. Dry Matter Content, Water Solubility and Density

The determinations of dry matter content and water solubility were conducted in accordance with the methods outlined by Yildiz et al. [21]. Film samples measuring $2 \times 2 \text{ cm}^2$ were initially weighed (W_1). These were dried at $105 \text{ }^\circ\text{C}$ until a constant weight was achieved (W_2). The dried samples were then dipped in 25 mL water at $25 \text{ }^\circ\text{C}$ for 24 h and subsequently dried again at $105 \text{ }^\circ\text{C}$ for 24 h. Finally, the samples were weighed (W_3) once again. The dry matter and water solubility were calculated using Equations (2) and (3), respectively.

$$\text{Dry matter(\%)} = 100 - \left[\frac{W_1 - W_2}{W_1} \times 100 \right] \quad (2)$$

$$\text{Solubility(\%)} = \frac{W_2 - W_3}{W_2} \times 100 \quad (3)$$

In accordance with the method outlined by Sun et al. [22], the density of the films was ascertained by dividing the weight of the films by their volume. This volume was determined by multiplying the area of the film by its thickness. All measurements were carried out in triplicate.

2.6. Color and Opacity

Color and opacity of films were evaluated in the CIE $L^*a^*b^*$ color space according to Díaz et al. [23]. The determinations were undertaken at three random points of three films in a spectrophotometer X-Rite (mod. SP60; Grand Rapids, MI, USA).

The difference in color (ΔE^*) of films regarding the WPI film's color values was calculated as follows:

$$\Delta E^* = \sqrt{(L^* - L_0)^2 + (a^* - a_0)^2 + (b^* - b_0)^2} \quad (4)$$

where L^* , a^* and b^* are the color values for the WS and SCW samples and L_0 , a_0 and b_0 are the color values for the WPI film.

The whiteness index of the films was calculated according to Saberi et al. [24] using the following formula:

$$\text{Whiteness index} = 100 - \sqrt{(100 - L^*)^2 + a^{*2} + b^{*2}} \quad (5)$$

The calculation of opacity values was conducted in accordance with Márquez-Reyes et al. [25], using Equation (6).

$$\text{Opacity(\%)} = \frac{Y_B}{Y_W} \times 100 \quad (6)$$

where Y_B is the opacity of the film against a black background and Y_W is the opacity of the film against a white background.

2.7. Mechanical Properties

The mechanical properties of films were determined using a texturometer model EZ Test and the Trapezium2 (version 1.03SP) data processing system software (Shimadzu Corporation, Tokyo, Japan), according to the method reported by Díaz et al. [23] based on the ASTM D882 method [26]. The samples of the films were cut and stored in a desiccator maintained at $20 \text{ }^\circ\text{C}$ with relative humidity of 45% for 48 h prior to testing.

2.8. Antioxidant Activity

In order to ascertain DPPH radical scavenging capacity, the procedure outlined by Vargas et al. [27] was followed. Film specimens (1 cm^2) were placed into tubes containing

4.0 mL of a 0.06 mM methanolic DPPH (2,2-diphenyl-1-picrylhydrazyl; Sigma-Aldrich, St. Louis, MO, USA) solution. The tubes were then maintained in conditions of darkness at a temperature of 25 °C for a period of two hours and thirty minutes. Following this, the film samples were separated, and the absorbances of the solutions were measured at 517 nm using a spectrophotometer (model 6850 UV/Vis; Jenway, Bibby Scientific, Stone, UK). Methanol was utilized as a blank. A calibration curve was prepared with DPPH [28] using concentrations of DPPH ranging from 0.006 mM to 0.06 mM in methanol. The determinations were carried out in duplicate. The antioxidant activity was expressed in terms of milligrams of DPPH degraded per gram of film weight and was calculated using Equation (7).

$$\text{Antioxidant activity (mg DPPH/g film)} = C \times \text{dilution rate/dry film weight in g} \quad (7)$$

where C is the value obtained from the calibration curve as mg of DPPH per mL of the difference between the absorbance of the DPPH reagent and the sample.

2.9. Fourier Transform Infrared Spectroscopy (FTIR)

The attenuated total reflection (ATR)–Fourier transform infrared (FTIR) spectra of the films were obtained by means of a Jasco FT/IR-4600 instrument equipped with the ATR Pro One accessory (manufactured by Jasco Corporation, Tokyo, Japan). The experimental determinations were conducted in triplicate. The spectra were measured between 400 and 4000 cm^{-1} by performing 16 scans at 1 cm^{-1} resolution. PeakFit software version 4.12 (SYSTAT Software, Richmond, CA, USA) was used to process the resulting data.

For the identification and intensity determination of individual band positions, the second derivative spectra were calculated on data previously baseline corrected and smoothed with a Savitsky–Golay function to remove possible noise.

2.10. Thermogravimetric Analysis (TGA)

Thermogravimetric analysis of the films was carried out in accordance with the method outlined by Díaz et al. [29]. Film samples (4.6–6.0 mg) were heated from 30 to 600 °C in an aluminum pan at a rate of 10 °C/min under a nitrogen atmosphere (30 mL/min). The measurements were carried out in duplicate. This analysis was performed using a thermogravimetric analyzer equipped with differential scanning calorimetry functionality (model TGA/DSC1; Mettler Toledo, Urdorf, Switzerland). The calculation of the first derivative of the TGA curve (DTG) was conducted by using PeakFit software (version 4.12; SYSTAT Software, Richmond, CA, USA).

2.11. Microstructure Analysis by Scanning Electron Microscopy (SEM)

An attenuated A JEOL-JSM 6360LV scanning electron microscope (Jeol, Ltd., Tokyo, Japan) operating at 15 kV was used to observe the microstructure of the films. The sample preparation was in accordance with the description of Díaz et al. [23].

2.12. X-Ray Diffraction (XRD)

The crystallinity of films was studied using an X-ray diffractometer (Bruker D8 Advance with a LYNXEYE XE-T detector, Bruker, Karlsruhe, Germany) with a $\text{CuK}\alpha 1$ radiation beam ($\lambda = 1.5406 \text{ \AA}$) in the angular range of 3 to 50 (2θ) at a voltage of 40 kV and current of 40 mA.

2.13. Statistical Analysis

The evaluation of data was conducted utilizing IBM SPSS Statistics for Windows version 28.0.1.0, developed by IBM Corporation (Armonk, NY, USA). Before statistical

analysis, the data were checked for outliers, and normal distribution was tested using the Kolmogorov–Smirnov test. One-way analysis of variance (ANOVA) and Tukey’s post hoc test were utilized for the purpose of testing and comparing, respectively, the statistical significance of differences among means. The statistical significance of differences in means was established with a significance level of $p < 0.05$. A two-way ANOVA was used to analyze the effects of the substitution of WPI by SCW and of the addition of oregano essential oil and their interaction on all of the determined parameters (only in samples with the WPI–SCW mixture: 2, 3, 4, 6, 7, 8, 9, 10, 11).

3. Results and Discussion

3.1. Visual Appearance

Figure 1 shows the visual appearance of the films. No important differences were observed among the films. Sajimon et al. [16] reported that films with high levels of oregano essential oil had a reddish tint. However, this was only observed in samples with 4% of essential oil. The addition of 2% of EO did not cause an unpleasant appearance of the films.

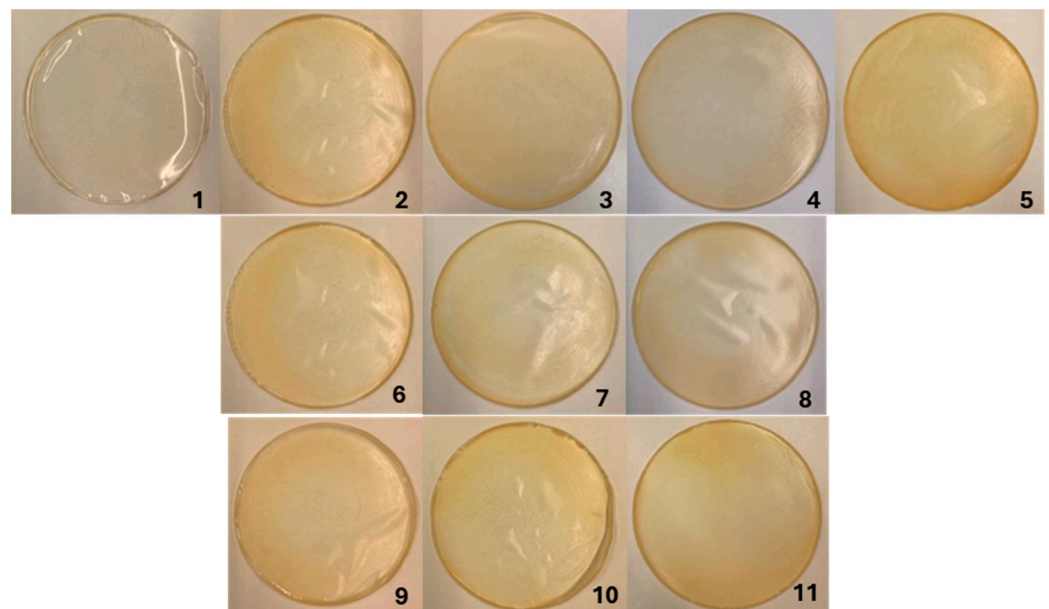


Figure 1. Visual appearance of the films described in the materials and methods section. (1) WPI; (2) WS 2:1; (3) WS 1:1; (4) WS 1:2; (5) SCW; (6) WS 2:1O1; (7) WS 1:1O1; (8) WS 1:2O1; (9) WS 2:1O2; (10) WS 1:1O2; (11) WS 1:2O2.

3.2. Water Vapor Permeability, Thickness, Dry Matter Content, Solubility and Density

Water vapor permeability (WVP), thickness, dry matter content, solubility and density values of films are shown in Table 1. Two-way ANOVA of these characteristics in films of WPI–SCW mixture are shown in Table 2. No significant effects of the substitution of WPI by SCW and the addition of EO were found in the water vapor permeability. However, the films produced with the addition of 2% of EO showed lower values of WVP than the corresponding films with the incorporation of 1% of EO and these samples showed lower values than films without EO. It has been reported that the addition of essential oils reduces the vapor permeability of the films due to that the incorporation of a hydrophobic agent, such as an essential oil, decreases the hydrophilic portion of the films and their affinity to the water and enhances their ability to act as a barrier to water vapor permeation [18,30,31]. A different result was observed by Oliveira et al. [17], one which indicated that the addition of oregano essential oil increased the WVP due to the oil not binding to the proteins,

leaving empty spaces through which water can permeate. Thus, the effects of the addition of oregano EO in the water permeability of the films are not clear.

Table 1. Water vapor permeability (WVP), thickness, dry matter (D.M.), solubility and density (mean \pm SD) of films described in the materials and methods section.

| Film | WVP (ng s ⁻¹ m ⁻¹ Pa ⁻¹) | Thickness μ m | Dry Matter (g/100 g) | Solubility (% D.M.) | Density (g/cm ³) |
|----------|---|----------------------|-------------------------|------------------------|---------------------------------|
| WPI | 0.156 \pm 0.04 | 150.67 \pm 58.66 | 57.77 \pm 0.9 a | 81.44 \pm 0.94 d | 1.43 \pm 0.15 a |
| WS 2:1 | 0.135 \pm 0.05 | 166.33 \pm 40.27 | 63.34 \pm 1.7 ab | 79.04 \pm 3.22 cd | 1.73 \pm 0.27 ab |
| WS 1:1 | 0.089 \pm 0.01 | 131.83 \pm 33.45 | 65.59 \pm 2.04 b | 78.86 \pm 2.85 cd | 2.07 \pm 0.06 ab |
| WS 1:2 | 0.104 \pm 0.03 | 172.33 \pm 40.55 | 66.69 \pm 2.24 b | 77.68 \pm 2.44 bcd | 1.49 \pm 0.23 a |
| SCW | 0.141 \pm 0.03 | 160.17 \pm 16.37 | 66.79 \pm 1.20 b | 66.49 \pm 3.64 a | 1.98 \pm 0.16 ab |
| WS 2:1O1 | 0.137 \pm 0.05 | 124.17 \pm 11.51 | 67.93 \pm 0.55 b | 71.54 \pm 0.99 ab | 3.27 \pm 0.06 b |
| WS 1:1O1 | 0.141 \pm 0.009 | 173.83 \pm 5.30 | 66.34 \pm 0.53 b | 74.59 \pm 0.27 abcd | 1.76 \pm 0.22 ab |
| WS 1:2O1 | 0.147 \pm 0.03 | 184.00 \pm 38.94 | 63.86 \pm 1.00 b | 74.05 \pm 1.95 abcd | 1.69 \pm 0.58 ab |
| WS 2:1O2 | 0.120 \pm 0.03 | 139.67 \pm 25.15 | 63.33 \pm 1.68 ab | 80.16 \pm 4.43 cd | 2.27 \pm 0.73 ab |
| WS 1:1O2 | 0.102 \pm 0.003 | 123.00 \pm 17.32 | 66.56 \pm 2.97 b | 74.12 \pm 6.64 abcd | 2.53 \pm 1.11 ab |
| WS 1:2O2 | 0.117 \pm 0.007 | 142.33 \pm 6.25 | 64.83 \pm 4.25 b | 68.48 \pm 2.98 ab | 2.11 \pm 0.96 ab |

Means in the same column with different letters (a–d) are significantly different ($p < 0.05$).

Table 2. Two-way ANOVA of water vapor permeability (WVP), thickness, dry matter, solubility and density of WS films.

| | | Two-Way ANOVA | |
|------------|--------------------|---------------|--------------|
| | | F | p Value |
| WVP | Proportion WPI/SCW | 0.98 | 0.393 |
| | Addition of OE | 3.40 | 0.056 |
| | Interaction | 0.69 | 0.609 |
| Thickness | WPI/SCW | 2.05 | 0.158 |
| | OE | 2.21 | 0.139 |
| | Interaction | 2.07 | 0.127 |
| Dry matter | WPI/SCW | 0.88 | 0.432 |
| | OE | 0.65 | 0.534 |
| | Interaction | 2.60 | 0.071 |
| Solubility | WPI/SCW | 2.57 | 0.104 |
| | OE | 6.01 | 0.010 |
| | Interaction | 3.65 | 0.024 |
| Density | WPI/SCW | 2.78 | 0.089 |
| | OE | 2.18 | 0.141 |
| | Interaction | 2.54 | 0.076 |

No significant effects of the substitution of WPI by SCW and the addition of EO were found in the thickness of the films. Other researchers have also indicated that the addition of essential oils did not modify the thickness of the films [32]. However, Sajimon et al. [16] have observed that the incorporation of oregano essential oil causes an increase in film thickness due to the way in which that addition causes disruption to the structure. This different result could be due to the different homogenizers used. No remarkable effects of the substitution of WPI by SCW or the addition of EO were found in density of the films. Despite the compositional differences between SCW and WPI (higher lipid and ash contents in SCW), the effective homogenization of the film-forming solutions likely maintained structural uniformity, preventing significant changes in the mass-to-volume ratio.

In relation to the dry matter content, it is remarkable that the films made only with WPI showed lower values of dry matter than the films with a mixture WPI–SCW or with only SCW. The dry matter content of the films was not influenced by the incorporation of

OE, though other researchers have indicated that essential oil addition can increase the dry matter content of the films [16,33].

Significant effects of the addition of EO and significant interactions between this incorporation and the substitution of WPI by SCW in the water solubility of the films were observed. In the films without EO, the addition of SCW caused a decrease in the water solubility of the films, with the films with only SCW showing significantly lower values than the other films. This result could be due to the way in which SCW has higher levels of fat than WPI and the way in which the hydrophobic properties of lipids can decrease the water solubility of the films. The water solubility of proteins is also related to the protein structure and the bonds among proteins [17]. The denatured state of the SCW proteins probably increased the amount of intermolecular disulfide bonds, which made the SCW films more resistant to solubilization in water. The substitution of WPI by SCW also significantly decreased the solubility of the films in the films with 2% of EO but this was not observed in films with 1% of EO. This different effect of the substitution of WPI by SCW in films with different concentration of EO should be investigated in future experiments. The films with the addition of oregano EO showed lower solubility than the films without EO, except in the film WS 2:1O2. The decrease of water solubility by the addition of oregano essential oil has also been observed in other works, and attributed to the hydrophobic properties of the lipids [16,17].

3.3. Color

The CIE $L^*a^*b^*$ color values, total color difference (ΔE), opacity and whiteness index are shown in Table 3. Two-way ANOVA of the color of the films with the WPI–SCW mixture are shown in Table 4. The substitution of WPI by SCW significantly influenced the color parameters. The addition of SCW to the films decreased the value of L^* but only in samples without essential oil. The substitution of WPI by SCW increased the values of a^* and b^* in the films with or without EO. Total color difference (ΔE) presented significant changes with the addition of SCW, with values of ΔE that are higher than 2. This indicates that inexperienced observers can detect differences in the films with different proportions of WPI and SCW [34]. The color parameters of the films (L^* , a^* , b^*) and their opacity were not influenced by the addition of EO. However, Sajimon et al. [16] observed that the incorporation of oregano essential oil decreased the lightness, whereas the influence in a^* and b^* are contradictory because it was found to depend on the amount of EO. The decrease of lightness was attributed to the fact that the oregano essential oil was included in small globules in the structure of the films. The different homogenizers in the preparation of the mixtures and the different brands used could influence both the distribution of EO and the color of the films.

Table 3. CIE $L^*a^*b^*$ color parameters, total color difference (ΔE), opacity and whiteness index (mean \pm SD) of the films described in the materials and methods section.

| Film | L^* | a^* | b^* | ΔE | Opacity | Whiteness |
|----------|---------------------|----------------------|----------------------|----------------------|----------------------|---------------------|
| WPI | 92.96 \pm 0.49 c | −3.04 \pm 0.09 ab | 3.15 \pm 2.04 a | 0.00 \pm 0.00 a | 14.91 \pm 0.25 a | 91.59 \pm 1.19 d |
| WS 2:1 | 90.08 \pm 1.35 b | −3.11 \pm 0.10 a | 7.04 \pm 1.59 ab | 4.92 \pm 2.18 ab | 18.55 \pm 0.22 b | 87.43 \pm 1.92 cd |
| WS 1:1 | 88.16 \pm 1.25 ab | −2.89 \pm 0.13 abc | 9.86 \pm 2.16 bcd | 8.33 \pm 4.13 bc | 22.00 \pm 1.18 de | 84.30 \pm 2.26 bc |
| WS 1:2 | 88.51 \pm 0.97 ab | −2.46 \pm 0.32 bc | 13.00 \pm 2.27 cd | 10.83 \pm 2.93 bcd | 26.82 \pm 0.59 g | 82.46 \pm 2.22 b |
| SCW | 86.16 \pm 1.32 a | −1.10 \pm 0.52 d | 18.11 \pm 2.21 e | 16.58 \pm 2.22 d | 23.81 \pm 1.79 ef | 77.17 \pm 2.48 a |
| WS 2:1O1 | 88.60 \pm 1.00 ab | −3.06 \pm 0.09 ab | 8.86 \pm 1.45 bc | 7.21 \pm 1.21 bc | 19.55 \pm 0.66 bcd | 85.17 \pm 0.40 bc |
| WS 1:1O1 | 88.52 \pm 0.62 ab | −2.92 \pm 0.17 ab | 11.60 \pm 1.33 bcd | 9.54 \pm 2.37 bc | 21.28 \pm 0.65 cde | 83.41 \pm 1.24 bc |
| WS 1:2O1 | 88.09 \pm 0.60 ab | −2.25 \pm 0.21 c | 14.67 \pm 1.68 de | 12.53 \pm 1.65 cd | 27.61 \pm 1.16 g | 80.96 \pm 1.59 ab |
| WS 2:1O2 | 88.82 \pm 0.74 b | −3.03 \pm 0.07 ab | 9.63 \pm 0.71 bc | 7.74 \pm 0.90 bc | 18.83 \pm 0.73 bc | 84.94 \pm 1.00 bc |
| WS 1:1O2 | 88.91 \pm 0.27 b | −2.85 \pm 0.15 abc | 11.52 \pm 1.07 bcd | 9.33 \pm 2.99 bc | 21.86 \pm 0.59 de | 83.75 \pm 0.84 bc |
| WS 1:2O2 | 88.44 \pm 0.12 ab | −2.58 \pm 0.16 abc | 13.15 \pm 1.54 cde | 11.01 \pm 1.70 bcd | 24.83 \pm 0.82 fg | 82.28 \pm 1.16 b |

Means in the same column with different letters (a–g) are significantly different ($p < 0.05$).

Table 4. Two-way ANOVA of color parameters of the WS films.

| Color Parameters | | Two-Way ANOVA | |
|------------------|-------------|---------------|--------------|
| | | F | p Value |
| L* | WPI/SCW | 2.24 | 0.135 |
| | OE | 0.82 | 0.455 |
| | Interaction | 1.27 | 0.317 |
| a* | WPI/SCW | 34.18 | 0.000 |
| | OE | 0.55 | 0.586 |
| | Interaction | 1.30 | 0.307 |
| b* | WPI/SCW | 22.78 | 0.000 |
| | OE | 3.08 | 0.071 |
| | Interaction | 0.56 | 0.698 |
| ΔE | WPI/SCW | 8.961 | 0.002 |
| | OE | 1.267 | 0.306 |
| | Interaction | 0.273 | 0.892 |
| Opacity | WPI/SCW | 207.33 | 0.000 |
| | OE | 3.54 | 0.050 |
| | Interaction | 4.24 | 0.014 |
| Whiteness | WPI-SCW | 15.03 | 0.000 |
| | OE | 2.43 | 0.117 |
| | Interaction | 0.56 | 0.693 |

3.4. Mechanical Properties

The mechanical properties of the films and the two-way ANOVA of these properties of the films with the WPI-SCW mixture are shown in Tables 5 and 6, respectively. All of these properties (tensile strength, elongation at break, elastic modulus, puncture strength and deformation and elastic modulus) were significantly influenced by the substitution of WPI by SCW. The films with SCW only and with the highest proportion of SCW showed the lowest values of tensile and puncture strengths, elongation at break and puncture deformation. These effects in the mechanical properties of the films could limit the use of the highest levels of SCW in the food industry. This could be because SCW has high levels of denatured proteins, soluble peptides, lactose and non-protein nitrogen [9].

Table 5. Mechanical properties (mean \pm SD) of films described in material and methods section.

| Film | Tensile Strength at Maximum (MPa) | Elongation at Break (%) | Puncture Strength (MPa) | Puncture Deformation (%) | Elastic Modulus (MPa) |
|----------|-----------------------------------|-------------------------|-------------------------|--------------------------|-----------------------|
| WPI | 1.57 \pm 0.73 ef | 52.17 \pm 17.32 ef | 2.40 \pm 0.66 e | 18.92 \pm 5.74 h | 7.41 \pm 2.08 a |
| WS 2:1 | 1.17 \pm 0.18 de | 57.26 \pm 14.77 ef | 1.74 \pm 0.14 d | 15.71 \pm 3.89 gh | 15.00 \pm 8.45 bc |
| WS 1:1 | 1.19 \pm 0.22 de | 45.20 \pm 9.83 de | 1.87 \pm 0.36 de | 9.57 \pm 2.40 def | 11.24 \pm 2.60 abc |
| WS 1:2 | 0.46 \pm 0.14 ab | 19.56 \pm 7.79 abc | 0.51 \pm 0.16 abc | 3.55 \pm 1.33 abc | 16.75 \pm 4.22 c |
| SCW | 0.17 \pm 0.05 a | 3.57 \pm 1.18 a | 0.20 \pm 0.03 a | 0.93 \pm 0.28 a | 9.25 \pm 4.13 ab |
| WS 2:1O1 | 1.02 \pm 0.25 cd | 30.32 \pm 9.27 bcd | 2.07 \pm 0.59 de | 12.34 \pm 2.42 fg | 12.29 \pm 3.04 abc |
| WS 1:1O1 | 0.61 \pm 0.12 abc | 34.32 \pm 10.99 cd | 0.94 \pm 0.11 bc | 7.62 \pm 1.11 cde | 8.07 \pm 2.99 a |
| WS 1:2O1 | 0.41 \pm 0.08 a | 15.01 \pm 4.65 ab | 0.47 \pm 0.11 ab | 2.56 \pm 0.95 ab | 7.09 \pm 1.54 a |
| WS 2:1O2 | 1.90 \pm 0.36 f | 68.22 \pm 14.30 f | 1.77 \pm 0.48 d | 11.14 \pm 3.47 ef | 14.66 \pm 3.27 bc |
| WS 1:1O2 | 0.95 \pm 0.16 bcd | 27.59 \pm 8.70 bc | 1.05 \pm 0.17 c | 5.52 \pm 0.94 bcd | 9.91 \pm 2.08 ab |
| WS 1:2O2 | 0.55 \pm 0.09 abc | 17.98 \pm 3.34 abc | 0.66 \pm 0.13 abc | 3.57 \pm 1.00 abc | 7.54 \pm 2.37 a |

Means in the same column with different letters (a-h) are significantly different ($p < 0.05$).

Table 6. Two-way ANOVA of mechanical properties of WS films.

| Mechanical Properties | | Two-Way ANOVA | |
|-----------------------|-------------|---------------|---------|
| | | F | p Value |
| TS | WPI/SCW | 104.22 | 0.000 |
| | OE | 28.09 | 0.000 |
| | Interaction | 14.07 | 0.000 |
| EB | WPI/SCW | 70.25 | 0.000 |
| | OE | 13.53 | 0.000 |
| | Interaction | 11.73 | 0.000 |
| PS | WPI/SCW | 112.63 | 0.000 |
| | OE | 3.88 | 0.026 |
| | Interaction | 11.03 | 0.000 |
| PD | WPI/SCW | 117.44 | 0.000 |
| | OE | 10.66 | 0.000 |
| | Interaction | 2.76 | 0.035 |
| EM | WPI/SCW | 8.12 | 0.000 |
| | OE | 11.12 | 0.000 |
| | Interaction | 3.47 | 0.013 |

TS—tensile strength, EB—elongation at break, PS—puncture strength, PD—puncture deformation, EM—elastic modulus.

The addition of EO also significantly influenced the mechanical properties of the films. It was observed that films with 1% of EO showed lower values of tensile strength and elongation at break than films without EO; however, the films with 2% EO showed higher values of tensile strength than the corresponding films with 1% EO. Sajimon et al. [16] observed the different evolution of these parameters, depending on the amount of oregano essential oil. They detected increases in tensile strength and elongation percentage with the addition of up to 2% of EO in WPI films, but that the incorporation of 3% decreased both values [16]. It has been observed that the addition of other essential oils increases the tensile strength and the elongation of the films [32,33,35,36] and has been explained by the way these compounds can become intercalated between the whey proteins, acting as plasticizers [32]. The incorporation of EO significantly decreased the values of puncture deformation of the films.

3.5. Antioxidant Activity

Table 7 shows the DPPH radical scavenging capacity of films. The two-way ANOVA of the DPPH radical scavenging capacity of the films with a WPI–SCW mixture are shown in Table 8. No significant effects of the substitution of WPI by SCW in the antioxidant activity of the films were observed. The addition of EO significantly increased the antioxidant activity of the films, as has been reported [16], being a very significant factor in the increase of the values (from 0.97–1.19 in samples without EO to 2.00–2.19 in films with 2% of EO). The samples with 2% of EO showed higher values than those with 1% of EO. The films with a WPI–SCW mixture with the highest concentration of EO could be very useful in foods with a high content of polyunsaturated fatty acids to reduce oxidation of the lipids.

Table 7. DPPH radical scavenging capacity (mean ± SD) of films described in material and methods section.

| Film | Antioxidant Activity (mg DPPH/g Film) |
|--------|---------------------------------------|
| WPI | 1.06 ± 0.27 a |
| WS 2:1 | 1.19 ± 0.31 a |

Table 7. Cont.

| Film | Antioxidant Activity (mg DPPH/g Film) |
|----------|---------------------------------------|
| WS 1:1 | 1.04 ± 0.16 a |
| WS 1:2 | 0.97 ± 0.16 a |
| SCW | 1.09 ± 0.13 a |
| WS 2:1O1 | 1.52 ± 0.18 abc |
| WS 1:1O1 | 1.35 ± 0.08 a |
| WS 1:2O1 | 1.48 ± 0.15 ab |
| WS 2:1O2 | 2.08 ± 0.21 cd |
| WS 1:1O2 | 2.00 ± 0.30 bcd |
| WS 1:2O2 | 2.19 ± 0.40 d |

Means with different letters (a–d) are significantly different ($p < 0.05$).

Table 8. Two-way ANOVA of the DPPH radical scavenging capacity of WS films.

| | | Two-Way ANOVA | |
|----------------------|-------------|---------------|--------------|
| Antioxidant Activity | | F | p Value |
| DPPH | WPI/SCW | 1.02 | 0.376 |
| | EO | 57.79 | 0.000 |
| | Interaction | 0.60 | 0.667 |

3.6. Fourier Transform Infrared Spectroscopy (FTIR)

FTIR spectra of films can be observed in Figures 2 and 3. Some bands corresponding to Amide I region ($1600\text{--}1700\text{ cm}^{-1}$) showed changes in the wave number (WN) in SCW-added films compared with WPI films. This region is governed by the stretching vibration of the C=O and C–N groups and provides information about the secondary structure of proteins [36]. Bands observed at $1610\text{--}1634\text{ cm}^{-1}$ and at $1675\text{--}1683\text{ cm}^{-1}$ correspond to β -sheet structures; bands at $1641\text{--}1646\text{ cm}^{-1}$ are attributed to random coil or unordered structure. The 1652 cm^{-1} band has been assigned to α -helix, and the $1660\text{--}1668\text{ cm}^{-1}$ and 1692 cm^{-1} bands to β -turn [37]. The mean values of each secondary structure were 56.9% β -sheet, 15.8% random coil, 10.6% α -helix and 16.7% β -turn. The β -sheet structure proportion was found to be higher than the values reported by other authors [36,38]. High levels of β -sheet structures are often observed in aggregate proteins, particularly those that have undergone extensive thermal denaturation [36] as in the case for samples to which SCW was added.

In bands corresponding to the β -sheet structure of proteins, several differences were found: the band at 1625 cm^{-1} in the WPI films shifted to a lower WN (1623 cm^{-1}) in WPI–SCW films. Furthermore, a new band at 1628 cm^{-1} was observed in the latter. Both bands have been assigned to the intramolecular β -sheet structure [37].

The band at 1643 cm^{-1} in WPI films also showed a shift to a lower WN in SCW-added films, 1640 cm^{-1} , in which another new band was found at 1646 cm^{-1} . The appearance of a new band corresponding to random coils has been observed after emulsion formation in caseins dispersions [39].

The spectral region from $2850\text{ to }2980\text{ cm}^{-1}$ is assigned to the stretching vibrations of the C–H bonds from methyl groups [36,40]. Two bands showed changes in their WN depending on the sample. The band at 2843 cm^{-1} in the WPI films shifted to a higher WN ($2850\text{--}2856\text{ cm}^{-1}$) in WPI–SCW films, with or without EO. By contrast, the band at 2932 cm^{-1} in the WPI films shifted to a lower WN ($2922\text{--}2925\text{ cm}^{-1}$) in films with SCW. These vibration frequencies have been assigned to the symmetrical and asymmetrical C–H stretching of $-\text{CH}_2$ from aliphatic chains, probably related to lipids [37,40]. The intensity of the bands in this spectral region increased in SCW- and EO-added samples compared with WPI films, probably due to the high lipid content of the SCW. However, the increment

of the number of $-CH_2$ vibrations could also be due to the decrease in the interactions between lipids and proteins. Changes in the 2922 cm^{-1} band have been related to emulsion stability [40].

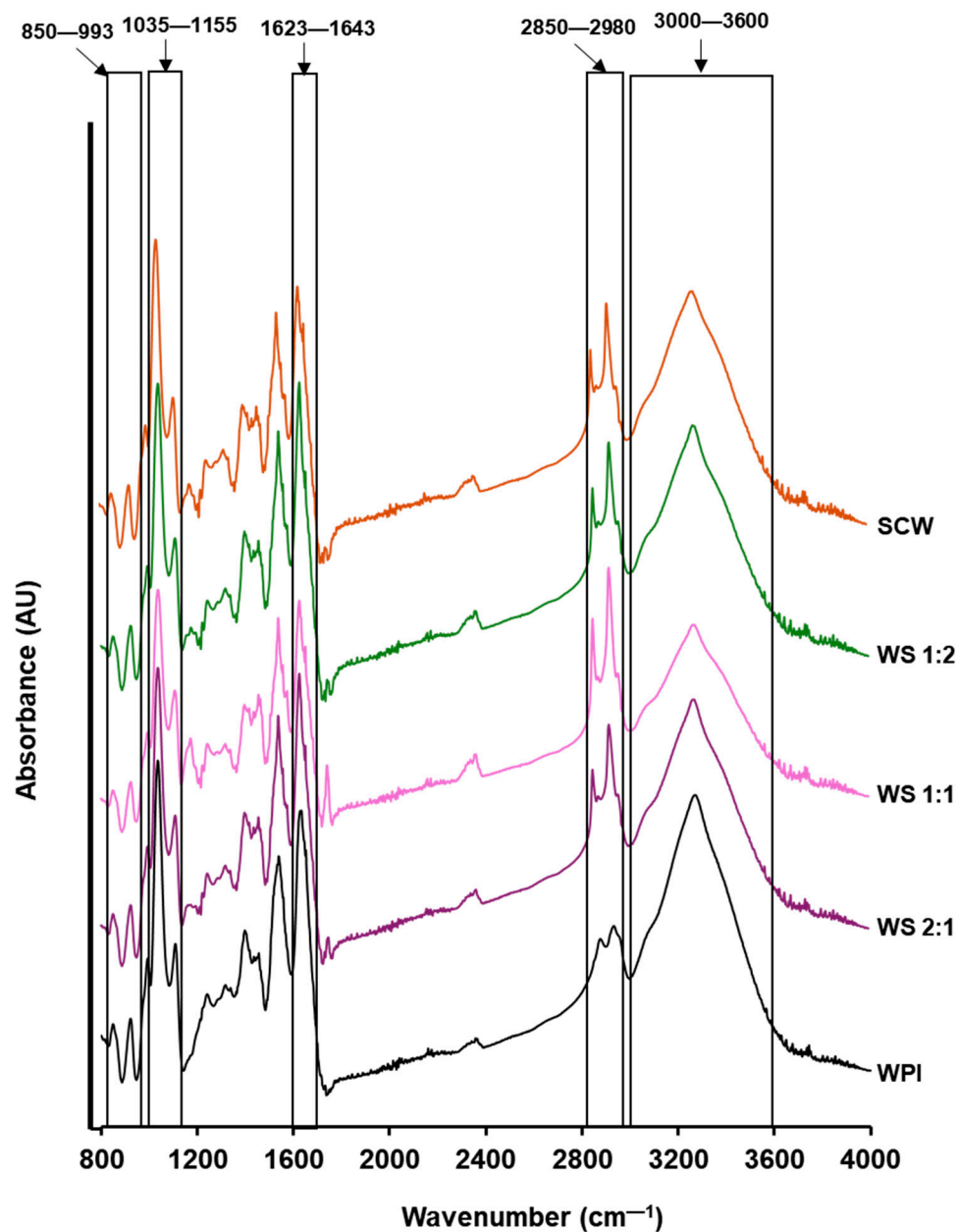


Figure 2. FTIR spectra of films with WPI and/or SCW described in the materials and methods section.

The absorption peaks located in the spectral range between 3000 cm^{-1} and 3600 cm^{-1} and are related to free and bound O–H and N–H groups [36]. There were no differences in band wave numbers, although the intensity of the peaks in this region was lower in WPI–SCW films (lesser O–H vibrations) than in the WPI samples. This result may be derived from a higher degree of interactions by hydrogen bonding in the protein network, which involve a reduction in the availability of free -OH groups [36].

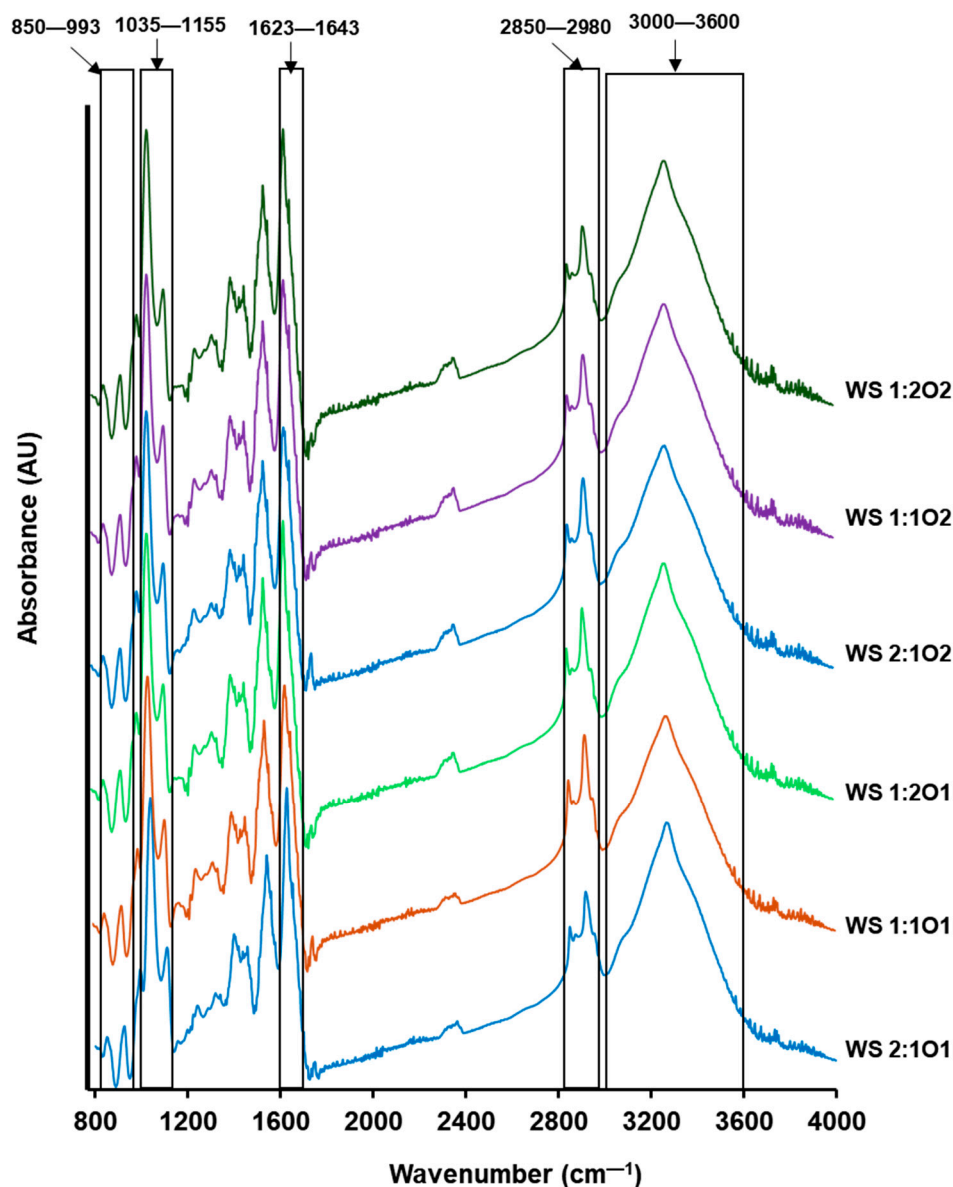


Figure 3. FTIR spectra of films with oregano essential oil described in the materials and methods section.

Several absorption bands of glycerol were found in the spectral range between 800 and 1150 cm^{-1} . The bands at 850, 921 and 993 cm^{-1} are assigned to the vibrations of the backbone C–C bond, and the band found at 1035 cm^{-1} corresponds to C–O in C1 and C3 [36,41]. The intensity of these bands decreased in films with SCW, which can be attributed to the decrease in the interactions among proteins and the plasticizer. Other bands were observed in this region. The band at 1075 cm^{-1} increased its intensity in films with SCW and is related to the C–O stretching band in C–OH [42], although the peaks at approximately 1080 cm^{-1} are commonly attributed to OH stretching of carbohydrates such as lactose [43]. The band at 975 cm^{-1} also increased intensity, which could be due to the interactions of protein with Na^+ in the SCW-added films. Both bands, together with the band at 1155 cm^{-1} that was only observed in the SCW-added samples, have also been related to interactions between protein and phosphate groups [42]. The SCW showed higher ash content than the WPI, so more interactions among proteins and minerals may be possible.

The addition of EO did not influence the FTIR spectra of the films; the intensity and wave numbers of bands, and new peaks due to EO were not observed. This lack

of modifications could be due to the low proportion of oregano essential oil added to film-forming solutions, which did not produce chemical changes; similar observations have been reported by other authors [44].

3.7. Thermogravimetric Analysis (TGA)

Thermogravimetric analysis (TGA) and the first derivative of TGA (DTG) plots of the thermal degradation pattern of protein films are shown in Figure 4. DTG curves of percent weight loss versus temperature are obtained from raw thermogravimetric data. Table 9 shows the weight loss and residual weight of the films. Four weight loss stages were observed, as has also been reported by other authors [45]. The first period was 32–120 °C and corresponded to the evaporation of free water and hydrogen-bonded water to the film matrix; weight loss was around 9.4%.

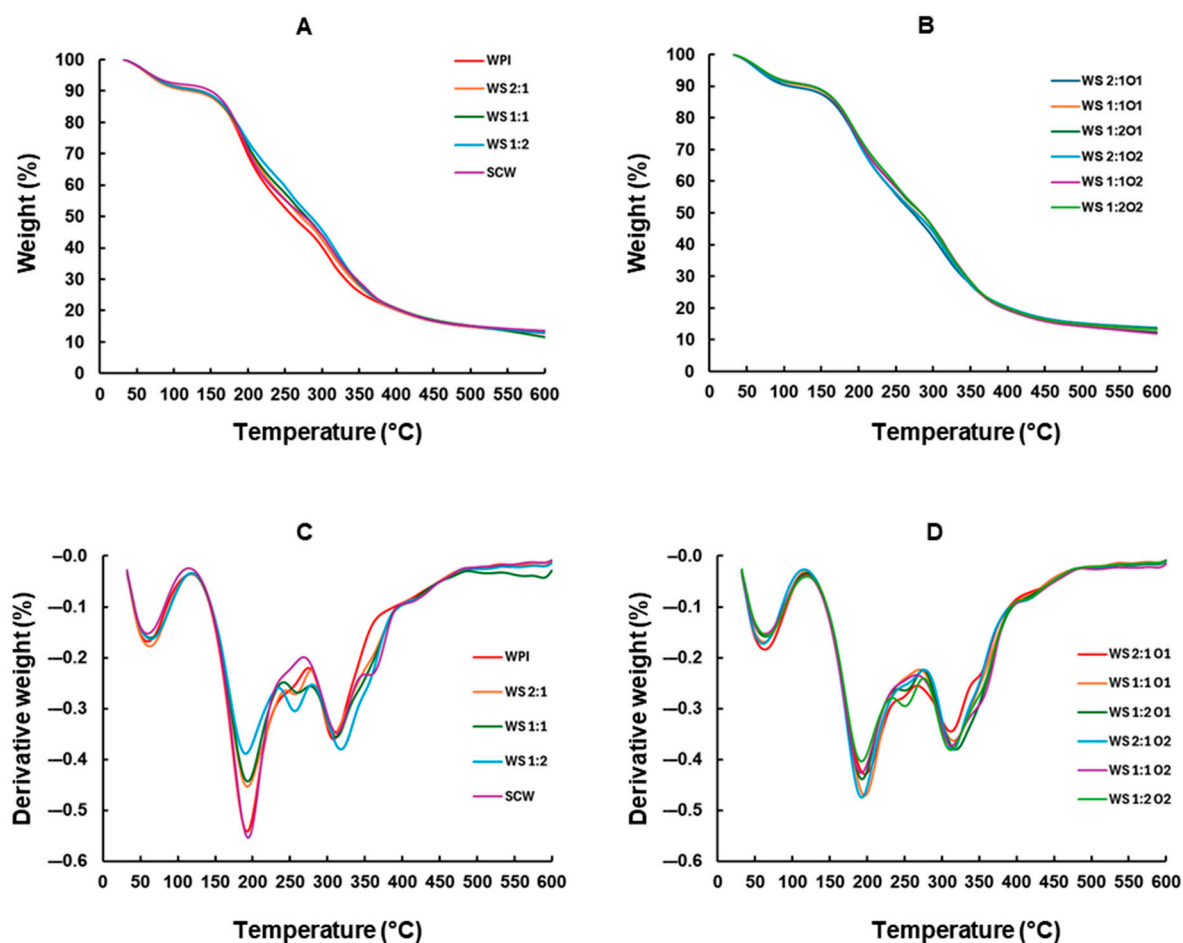


Figure 4. Thermogravimetric analysis (TGA) (A,B) and first derivative of TGA (DTG) (C,D) curves of the films described in the materials and methods section.

Table 9. Thermal degradation of the films described in the materials and methods section—weight loss and residual weight (%).

| Film | Stage I 32–120 °C | Stage II 120–235 °C | Stage III 235–370 °C | Stage IV 370–600 °C | Total Weight Loss | Residual Weight |
|--------|----------------------|------------------------|-------------------------|------------------------|-------------------------|--------------------|
| WPI | 9.21 | 34.76 | 33.38 | 10.55 | 87.28 | 12.72 |
| WS 2:1 | 9.94 | 31.24 | 35.41 | 10.58 | 86.70 | 13.30 |
| WS 1:1 | 9.39 | 28.64 | 36.57 | 13.05 | 88.64 | 11.36 |

Table 9. *Cont.*

| Film | Stage I 32–120 °C | Stage II 120–235 °C | Stage III 235–370 °C | Stage IV 370–600 °C | Total Weight Loss | Residual Weight |
|----------|----------------------|------------------------|-------------------------|------------------------|-------------------------|--------------------|
| WS 1:2 | 9.42 | 26.70 | 39.22 | 11.39 | 87.19 | 12.81 |
| SCW | 8.09 | 32.55 | 34.09 | 11.02 | 86.44 | 13.56 |
| WS 2:1O1 | 10.49 | 28.70 | 36.49 | 9.76 | 86.34 | 13.66 |
| WS 1:1O1 | 9.57 | 30.79 | 36.57 | 10.10 | 86.79 | 13.21 |
| WS 1:2O1 | 9.21 | 28.01 | 38.65 | 10.91 | 87.68 | 12.32 |
| WS 2:1O2 | 9.22 | 30.31 | 36.35 | 10.30 | 86.65 | 13.35 |
| WS 1:1O2 | 9.13 | 28.64 | 38.44 | 11.55 | 88.20 | 11.80 |
| WS 1:2O2 | 9.20 | 27.32 | 39.38 | 10.40 | 86.72 | 13.28 |

The second period occurred in the range of 120–235 °C and involved the thermal decomposition of glycerol, the degradation of low molecular weight compounds (including essential oils) and the vaporization of structure-bound water within the film [44]. The lowest weight losses were observed in WS films compared with WPI and SCW samples, and they were lower at the highest SCW proportion; interactions among WPI and SCW compounds (denatured proteins, lipids) may improve the thermal stability of WS films. The weight loss at the third stage (235–370 °C) was primarily caused by polymer degradation. The highest weight loss was found in WS 1:2 films. The fourth period was in the range of 370–600 °C; polymer carbonization was responsible for the weight loss above 370 °C.

Total weight loss was in the range of 86.3–88.6%, and the residual weight between 11.3% and 13.7%. The films with the highest values of residual weight were the mixture of WPI–SCW in a 2:1 proportion (WS 2:1) and the presence of EO did not modify this parameter. EO addition did not influence the weight loss of films.

Table 10 shows the temperature peaks observed at each stage. Three peaks were observed at around 63 °C, 193 °C and 313 °C in all of the films. Nevertheless, two peaks (at 257 °C and 313 °C) were only found at the third stage in the WS films, which involved the presence of two chain structures with different thermal stabilities. The peak at around 313 °C appeared in all samples and may correspond to the degradation of parts of the protein matrix in which molecules established better molecular interactions. The peak at 257 °C in the polymer degradation stage could indicate a lower thermal stability of films when SCW was added to WPI, which may be due to the degradation of the denatured proteins from the second cheese whey protein concentrate that interacted with whey proteins from WPI. This peak was found at lower temperatures, 246–252 °C, in WS films with EO. The interaction of EO with SCW and WPI proteins may cause this decrease. However, weight losses were similar in all samples, as mentioned above. Further studies are needed for the determination of the positive or negative influence of SCW and EO addition on the thermal stability of WPI in view of the industrial application of these films in food packaging.

Table 10. Thermal degradation of the films described in the materials and methods section—temperature peaks (°C).

| Film | Stage I 32–120 °C | Stage II 120–235 °C | Stage IIIa 235–370 °C | Stage IIIb 235–370 °C |
|----------|----------------------|------------------------|--------------------------|--------------------------|
| WPI | 62.7 | 193.0 | nd | 308.1 |
| WS 2:1 | 62.3 | 192.8 | 257.3 | 307.8 |
| WS 1:1 | 63.5 | 193.2 | 257.4 | 311.3 |
| WS 1:2 | 63.8 | 190.6 | 257.3 | 318.3 |
| SCW | 61.1 | 194.0 | nd | 312.5 |
| WS 2:1O1 | 63.6 | 195.9 | 246.2 | 311.9 |

Table 10. Cont.

| Film | Stage I 32–120 °C | Stage II 120–235 °C | Stage IIIa 235–370 °C | Stage IIIb 235–370 °C |
|----------|----------------------|------------------------|--------------------------|--------------------------|
| WS 1:1O1 | 62.2 | 197.0 | 247.2 | 315.8 |
| WS 1:2O1 | 65.4 | 193.1 | 249.9 | 316.8 |
| WS 2:1O2 | 61.2 | 192.6 | 251.3 | 314.4 |
| WS 1:1O2 | 64.4 | 193.4 | 251.7 | 314.4 |
| WS 1:2O2 | 66.1 | 192.3 | 250.3 | 312.5 |

nd, not detected.

3.8. Microstructure

Scanning electron microscopy was used to analyze the film microstructure. Figure 5 shows the surface images of experimental films. The WPI film surface was smooth, uniform and dense, while SCW films displayed a rough surface with aggregates of different sizes, probably due to the presence of denatured proteins and lipids. The WS films showed pinholes and cavities probably caused by lipid droplets from the SCW powder used in film-forming solutions; these droplets increased their size, and their distribution was more irregular proportionally to the amount of SCW in the mixture. When EO was added, more parts of the images appeared in a darker color compared with other sites of the film images; similar observations have been reported in WPI films containing free thyme extract [46].

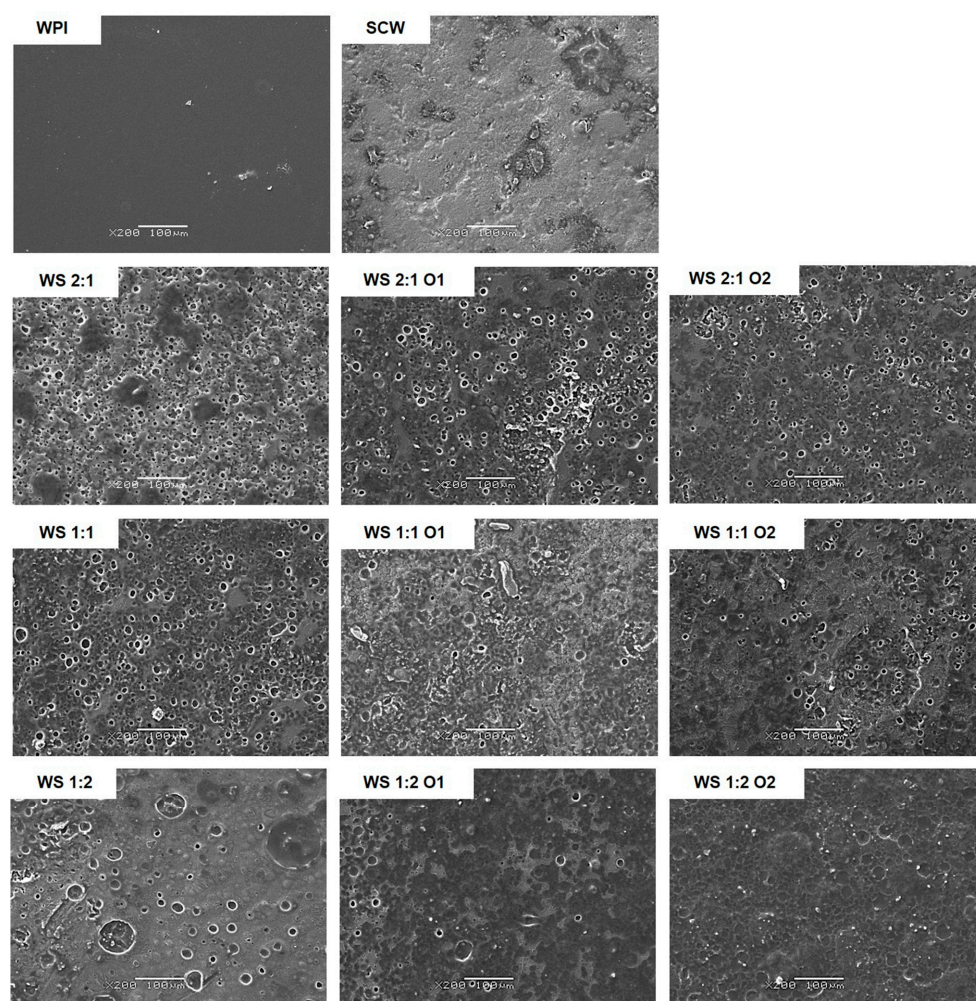


Figure 5. Surface image of the films described in the materials and methods section. Scale: 100 μm; magnification ×200.

Figure 6 presents the cross-sectional images of the films. The WPI films exhibited a rough and compact image due to the protein aggregates that formed the film matrix. The SCW films

showed a coarser appearance with cavities, due to the presence of highly denatured proteins. The WS 2:1 samples had a compact structure with small, sinuous creases. The increase of SCW content made the cross-sectional morphology of films rougher with larger aggregates, particularly in the WS 1:2 films. This phenomenon may be associated with the diminution of tensile strength and elongation values in films with higher proportions of SCW. In the case of the WS 1:2 films, the large aggregates were likely formed by denatured proteins from SCW, thereby impairing the mechanical properties of these films.

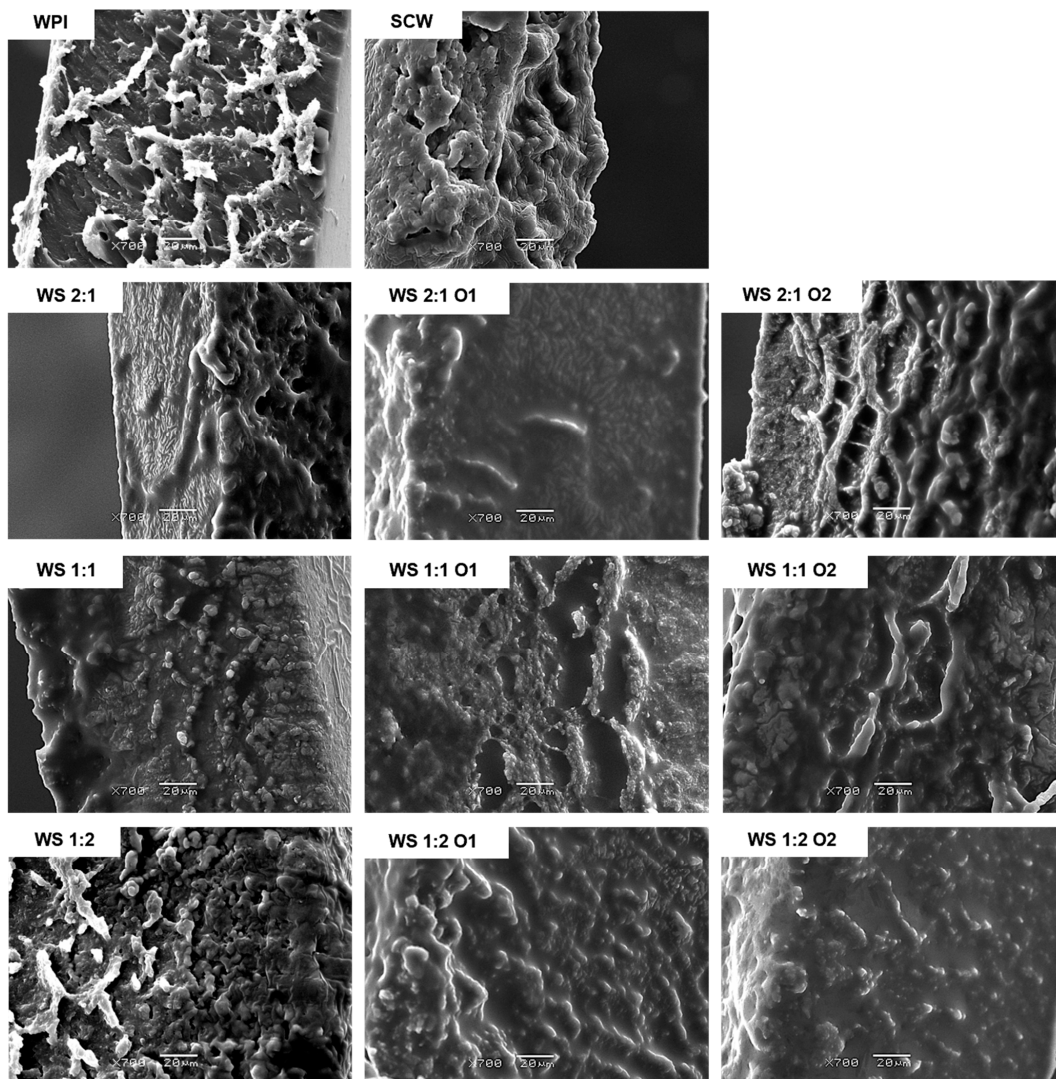


Figure 6. Cross-sectional images of the films described in the materials and methods section. Scale: 20 μm ; magnification $\times 700$.

The addition of EO modified the microstructure of the films. Larger aggregates and an increase in void sizes were observed in the WS 2:1 O2 and in the WS 1:1 and WS 2:1 films at both EO concentrations. The increase in roughness in protein films added with essential oils has been attributed to the attraction among the matrix components and EO, which at high concentrations can lead to the formation of agglomerates [44]. However, the nature of these interactions is likely to vary depending on the structural characteristics of the proteins involved. In the WS 2:1 O2 films, the presence of trabeculae that intersect voids was observed. These structures are likely the result of the interaction between WPI proteins and EO molecules, potentially contributing to enhanced mechanical properties, such as tensile strength and elongation, in comparison with the WS 2:1 and WS 2:1 O1 films. As previously documented by other researchers, an enhancement of these properties was observed when

increasing concentrations of essential oil were added [44]. The aforementioned effect was not observed in films with lower WPI content, likely due to the EO concentration exceeding the limit over which WPI proteins can interact with EO components. It is possible that denatured SCW proteins exhibited a diminished capacity for binding EO compounds due to changes in their structure.

3.9. X-Ray Diffraction (XRD)

As illustrated in Figure 7A, the diffractograms of the films WPI, SCW, and the mixtures of both (WS) reveal the occurrence of structural changes in two angular zones, depending on the sample. These changes may involve inter- or intra-molecular contacts of the polymeric chains or aggregates that become crystalline, as evidenced by the observation of peaks rather than bands. The low-angle zone, which corresponds to peaks and bands at 2θ in the range of 3° to 15° , shows the structural changes in the films. The diffractograms of the WPI films exhibit a poorly structured system, while the addition of SCW at varying proportions (all WS films) results in the formation of crystalline structures with peaks at 3.8° , 5.8° , and 9.8° . In the high angle disturbance zone (15° to 30°), the WS 1:2 and SCW films exhibit variations indicative of a higher degree of structuring, suggesting enhanced homogeneity in the inter- or intra-molecular contacts. Denaturing agents, such as heating, produce conformational changes in whey proteins that can induce the formation of novel peaks in diffractograms, as has been reported by other authors [47]. The addition of SCW powder to film-forming solutions involves the incorporation of denatured whey proteins that may affect the crystalline structure of films.

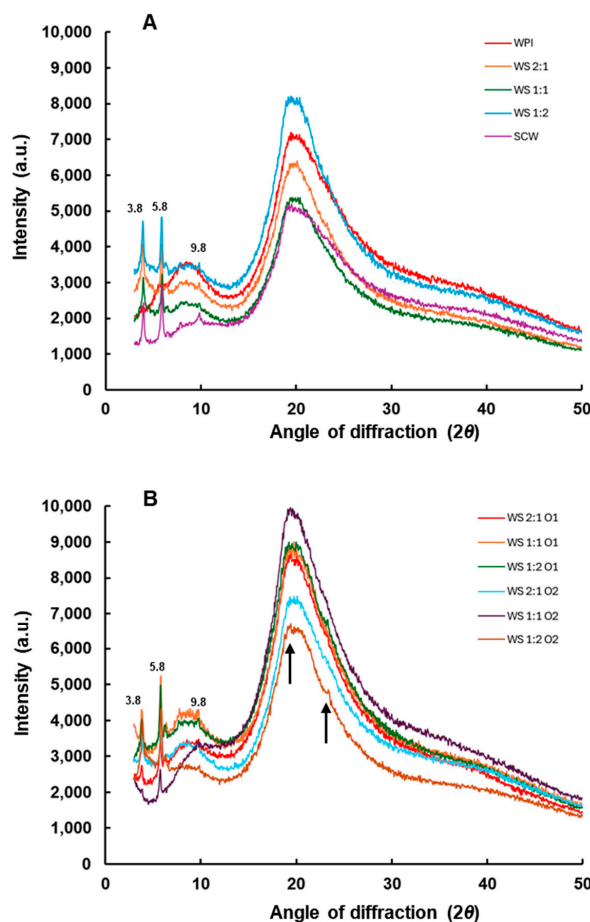


Figure 7. XRD patterns for the films with WPI and/or SCW (A) and the films with oregano essential oil (B) described in the materials and methods section. For arrows explanation see text.

The diffractograms of the WS films to which oregano essential oil was added are shown in Figure 7B. In the low-angle zone, peaks showing a crystalline component are also observed in all of the samples, as has been mentioned above. In the WS 1:2 films with added EO, the relative intensities of peaks 3.8, 5.8 and 9.8° were found to be higher than in the WS 1:2 sample without any addition. Furthermore, in the high-angle zone, two small peaks (indicated by arrows in Figure 7B) appear in the WS 1:2 O1 and O2 films. It may be possible that the essential oil interacted with the denatured whey proteins, present in greater proportion in these samples, and increased the crystallinity of the films. Amjadi et al. [48] have reported that the incorporation of orange peel essential oil improves the crystallinity of WPI-based films.

4. Conclusions

SCW powder, a by-product resulting from ovine whey cheese production, when combined with WPI, may be used to prepare edible films, but they showed important differences in their properties depending on the proportion of each product. The films with only SCW or a high proportion of SCW had the lowest values in tensile strength, elongation at break, puncture strength and puncture deformation. These effects in the mechanical properties of the films could limit the application of the highest levels of SCW in foods. The addition of oregano essential oil to the SCW–WPI films is useful to increase the antioxidant activity of the films, though it must also be considered that it can modify the water solubility and the mechanical properties of these films. The mixture of WPI and SCW at a 2:1 proportion, with the addition of 2% oregano essential oil, yielded films that exhibited the highest values of tensile strength and elasticity, and good antioxidant capacity. Consequently, these films can be regarded as the most efficient films for food packaging among those examined in this study. However, in view of their practical application, it is necessary to investigate other important parameters that affect their properties, such as the pH of the film-forming solutions, the incorporation of alternative plasticizers or the drying temperature, to improve their characteristics.

Author Contributions: Conceptualization, A.P., A.C., C.P. and O.D.; methodology, A.P. and O.D.; validation, A.P., A.C. and O.D.; formal analysis, A.C. and O.D.; investigation, A.P. and O.D.; resources, A.C., C.P. and O.D.; writing—original draft preparation, A.P., A.C. and O.D.; writing—review and editing, A.P., A.C., C.P. and O.D.; visualization, A.C. and O.D.; supervision, A.C., C.P. and O.D.; project administration, A.C. and O.D.; funding acquisition, A.C. and O.D. All authors have read and agreed to the published version of the manuscript.

Funding: This research was funded by Xunta de Galicia, grant number GPC ED431B 2019/13 and Ministerio de Ciencia e Innovación (Spain), grant number PID2019-107542RB-C21.

Institutional Review Board Statement: Not applicable.

Informed Consent Statement: Not applicable.

Data Availability Statement: The data presented in this work are available upon request from the corresponding author.

Acknowledgments: The authors wish to express thanks to RIAIDT-USC for the use of their analytical facilities.

Conflicts of Interest: The authors declare no conflicts of interest.

Abbreviations

The following abbreviations are used in this manuscript:

| | |
|------|---|
| SCW | Second cheese whey |
| EO | Essential oil |
| WPI | Whey protein isolate |
| WVP | Water vapor permeability |
| FTIR | Fourier transform infrared spectroscopy |
| TGA | Thermogravimetric analysis |
| XRD | X-ray diffraction |

References

1. Nilsson, F.; Silva, N.; Schelin, J. Single-use versus reusable packaging for perishable liquid foods-Exploring evidence from research on climate impact and food safety. *Resour. Conserv. Recycl.* **2024**, *207*, 107655. [CrossRef]
2. Pires, A.F.; Díaz, O.; Cobos, A.; Pereira, C.D. A review of recent developments in edible films and coatings-focus on whey-based materials. *Foods* **2024**, *13*, 2638. [CrossRef]
3. The European Parliament and the Council of the European Union. Regulation (EU) 2025/40 of 19 December 2024 on Packaging and Packaging Waste, Amending Regulation (EU) 2019/1020 and Directive (EU) 2019/904, and Repealing Directive 94/62/EC. Official Journal of the European Union, 22nd January 2025. Available online: <http://data.europa.eu/eli/reg/2025/40/oj> (accessed on 3 April 2025).
4. Gaspar, M.C.; Braga, M.E. Edible films and coatings based on agrifood residues: A new trend in the food packaging research. *Curr. Opin. Food Sci.* **2023**, *50*, 101006. [CrossRef]
5. Chen, H.; Wang, J.; Cheng, Y.; Wang, C.; Liu, H.; Bian, H.; Pan, Y.; Sun, J.; Han, W. Application of protein-based films and coatings for food packaging: A review. *Polymers* **2019**, *11*, 2039. [CrossRef] [PubMed]
6. Kandasamy, S.; Yoo, J.; Yun, J.; Kang, H.-B.; Seol, K.-H.; Kim, H.-W.; Ham, J.-S. Application of whey protein-based edible films and coatings in food industries: An updated overview. *Coatings* **2021**, *11*, 1056. [CrossRef]
7. Soliman, E.; Furuta, M. Influence of γ -irradiation on mechanical and water barrier properties of corn protein-based films. *Radiat. Phys. Chem.* **2009**, *78*, 651–654. [CrossRef]
8. Xu, J.; Li, Y. Wheat gluten-based coatings and films: Preparation, properties, and applications. *J. Food Sci.* **2023**, *88*, 582–594. [CrossRef] [PubMed]
9. Pires, A.F.; Marnotes, N.G.; Rubio, O.D.; Garcia, A.C.; Pereira, C.D. Dairy by-products: A review on the valorization of whey and second cheese whey. *Foods* **2021**, *10*, 1067. [CrossRef]
10. Etxabide, A.; Arregi, M.; Cabezudo, S.; Guerrero, P.; de la Caba, K. Whey protein films for sustainable food packaging: Effect of incorporated ascorbic acid and environmental assessment. *Polymers* **2023**, *15*, 387. [CrossRef]
11. Galus, S.; Kadzińska, J. Whey protein edible films modified with almond and walnut oils. *Food Hydrocoll.* **2016**, *52*, 78–86. [CrossRef]
12. Alfano, A.; D'ambrosio, S.; Cimini, D.; Falco, L.; D'Agostino, M.; Finamore, R.; Schiraldi, C. No waste from waste: Membrane-based fractionation of second cheese whey for potential nutraceutical and cosmeceutical applications, and as renewable substrate for fermentation processes development. *Fermentation* **2022**, *8*, 514. [CrossRef]
13. Pires, A.; Pietruszka, H.; Božek, A.; Szkolnicka, K.; Gomes, D.; Díaz, O.; Cobos, A.; Pereira, C. Sheep's Second Cheese Whey Edible Coatings with Oregano and Clary Sage Essential Oils Used as Sustainable Packaging Material in Cheese. *Foods* **2024**, *13*, 674. [CrossRef] [PubMed]
14. Seydim, A.C.; Sarikus-Tutal, G.; Sogut, E. Effect of whey protein edible films containing plant essential oils on microbial inactivation of sliced Kasar cheese. *Food Packag. Shelf Life* **2020**, *26*, 100567. [CrossRef]
15. Seydim, A.C.; Sarikus, G. Antimicrobial activity of whey protein based edible films incorporated with oregano, rosemary and garlic essential oils. *Food Res. Int.* **2006**, *39*, 639–644. [CrossRef]
16. Sajimon, A.; Edakkadan, A.S.; Subhash, A.J.; Ramya, M. Incorporating oregano (*Origanum vulgare* L.) Essential oil onto whey protein concentrate based edible film towards sustainable active packaging. *J. Food Sci. Technol.* **2023**, *60*, 2408–2422. [CrossRef]
17. Oliveira, S.P.L.F.; Bertan, L.C.; De Rensis, C.M.V.B.; Bilck, A.P.; Vianna, P.C.B. Whey protein-based films incorporated with oregano essential oil. *Polímeros* **2017**, *27*, 158–164. [CrossRef]
18. Çakmak, H.; Özselek, Y.; Turan, O.Y.; Firatlıgil, E.; Karbancıoğlu-Güler, F. Whey protein isolate edible films incorporated with essential oils: Antimicrobial activity and barrier properties. *Polym. Degrad. Stab.* **2020**, *179*, 109285. [CrossRef]
19. Cobos, Á.; Díaz, O. Impact of nanoclays addition on chickpea (*Cicer arietinum* L.) flour film properties. *Foods* **2024**, *13*, 75. [CrossRef]

20. ASTM. E 96-93—Standard test method for water vapor transmission of materials. In *Annual Book of ASTM Standard*; American Society for Testing and Materials: Philadelphia, PA, USA, 1993; pp. 701–708.
21. Yildiz, E.; Emir, A.A.; Sumnu, G.; Kahyaoglu, L.N. Citric acid cross-linked curcumin/chitosan/chickpea flour film: An active packaging for chicken breast storage. *Food Biosci.* **2022**, *50*, 102121. [[CrossRef](#)]
22. Sun, L.; Sun, J.; Chen, L.; Niu, P.; Yang, X.; Guo, Y. Preparation and characterization of chitosan film incorporated with thinned young apple polyphenols as an active packaging material. *Carbohydr. Polym.* **2017**, *163*, 81–91. [[CrossRef](#)]
23. Díaz, O.; Candia, D.; Cobos, A. Effects of ultraviolet radiation on properties of films from whey protein concentrate treated before or after film formation. *Food Hydrocoll.* **2016**, *55*, 189–199. [[CrossRef](#)]
24. Saberi, B.; Thakur, R.; Voung, Q.V.; Chockchaisawasdee, S.; Golding, J.B.; Scarlett, C.J.; Stathopoulos, C.E. Optimization of physical and optical properties of biodegradable edible films based on pea starch and guar gum. *Ind. Crops Prod.* **2016**, *86*, 342–352. [[CrossRef](#)]
25. Márquez-Reyes, J.M.; Rodríguez-Quiroz, R.E.; Hernández-Rodríguez, J.P.; Rodríguez-Romero, B.A.; Flores-Breceda, H.; Napoles-Armenta, J.; Romero-Soto, I.C.; Galindo-Rodríguez, S.A.; Báez-González, J.G.; Treviño-Garza, M.Z. Production and characterization of biocomposite films of bacterial cellulose from kombucha and coated with chitosan. *Polymers* **2022**, *14*, 3632. [[CrossRef](#)]
26. ASTM. D882—Standard test method for tensile properties of thin plastic sheeting. In *Annual Book of ASTM Standard*; American Society for Testing and Materials: Philadelphia, PA, USA, 2000; pp. 160–168.
27. Vargas, C.V.; Costa, T.M.H.; Rios, A.O.; Flores, S.H. Comparative study on the properties of films based on red rice (*Oryza glaberrima*) flour and starch. *Food Hydrocoll.* **2017**, *65*, 96–106. [[CrossRef](#)]
28. Kocakulak, S.; Sumnu, G.; Sahin, S. Chickpea flour-based biofilms containing gallic acid to be used as active edible films. *J. Appl. Polym. Sci.* **2019**, *136*, 47704. [[CrossRef](#)]
29. Díaz, O.; Ferreira, T.; Rodríguez-Otero, J.L.; Cobos, A. Characterization of chickpea (*Cicer arietinum* L.) flour films: Effects of pH and plasticizer concentration. *Int. J. Mol. Sci.* **2019**, *20*, 1246. [[CrossRef](#)]
30. Lee, J.H.; Lee, J.; Bin Song, K. Development of a chicken feet protein film containing essential oils. *Food Hydrocoll.* **2015**, *46*, 208–215. [[CrossRef](#)]
31. Christaki, S.; Moschakis, T.; Kyriakoudi, A.; Biliaderis, C.G.; Mourtzinos, I. Recent advances in plant essential oils and extracts: Delivery systems and potential uses as preservatives and antioxidants in cheese. *Trends Food Sci. Technol.* **2021**, *116*, 264–278. [[CrossRef](#)]
32. Pedro, S.; Pereira, L.; Domingues, F.; Ramos, A.; Luís, Â. Optimization of whey protein-based films incorporating *Foeniculum vulgare* Mill. essential oil. *J. Funct. Biomater.* **2023**, *14*, 121. [[CrossRef](#)]
33. Mahdavi, V.; Hosseini, S.E.; Sharifan, A. Effect of edible chitosan film enriched with anise (*Pimpinella anisum* L.) essential oil on shelf life and quality of the chicken burger. *Food Sci. Nutr.* **2018**, *6*, 269–279. [[CrossRef](#)]
34. Mokrzycki, W.S.; Tatol, M. Colour difference ΔE —A survey. *Mach. Graph. Vis.* **2011**, *20*, 383–411.
35. Ghoshal, G.; Shivani. Thyme essential oil nano-emulsion/Tamarind starch/Whey protein concentrate novel edible films for tomato packaging. *Food Control* **2022**, *138*, 108990. [[CrossRef](#)]
36. Ramos, O.L.; Reinas, I.; Silva, S.I.; Fernandes, J.C.; Cerqueira, M.A.; Pereira, R.N.; Vicente, A.A.; Pocas, M.F.; Pintado, M.E.; Malcata, F.X. Effect of whey protein purity and glycerol content upon physical properties of edible films manufactured therefrom. *Food Hydrocoll.* **2013**, *30*, 110–122. [[CrossRef](#)]
37. Stuart, B. *Infrared Spectroscopy: Fundamentals and Applications*; John Wiley & Sons: Chichester, UK, 2004; pp. 137–165.
38. Pereira, R.M.; Souza, B.W.S.; Cerqueira, M.A.; Teixeira, J.A.; Vicente, A.A. Effects of electric fields on protein unfolding and aggregation: Influence on edible films formation. *Biomacromolecules* **2010**, *11*, 2912–2918. [[CrossRef](#)]
39. Daniloski, D.; McCarthy, N.A.; Auldist, M.J.; Vailjevic, T. Properties of sodium caseinate as affected by the β -casein phenotypes. *J. Colloid Interface Sci.* **2022**, *626*, 939–950. [[CrossRef](#)] [[PubMed](#)]
40. Dinache, A.; Tozar, T.; Smarandache, A.; Andrei, I.R.; Nistorescu, S.; Nastasa, V.; Staicu, A.; Pascu, M.L.; Romanitan, M.O. Spectroscopic characterization of emulsions generated with a new laser-assisted device. *Molecules* **2020**, *25*, 1729. [[CrossRef](#)]
41. Matsakidou, A.; Tsimidou, M.Z.; Kiosseoglou, V. Storage behavior of caseinate-based films incorporating maize germ oil bodies. *Food Res. Int.* **2019**, *116*, 1031–1040. [[CrossRef](#)]
42. Arrieta, M.P.; Peltzer, M.A.; Garrigós, M.C.; Jiménez, A. Structure and mechanical properties of sodium and calcium caseinate edible active films with carvacrol. *J. Food Eng.* **2013**, *114*, 486–494. [[CrossRef](#)]
43. Andrade, J.; Pereira, C.G.; Junior, J.C.A.; Viana, C.C.R.; Neves, L.N.O.; da Silva, P.H.F.; Bell, M.J.V.; dos Anjos, V.C. FTIR-ATR determination of protein content to evaluate whey protein concentrate adulteration. *LWT Food Sci. Technol.* **2019**, *99*, 166–172. [[CrossRef](#)]
44. Wang, K.; Wang, Y.; Cheng, M.; Wang, Y.; Zhao, P.; Xi, X.; Lu, J.; Wang, X.; Han, X.; Wang, J. Preparation and characterization of active films based on oregano essential oil microcapsules/soybean protein isolate/sodium carboxymethyl cellulose. *Int. J. Biol. Macromol.* **2024**, *258*, 128985. [[CrossRef](#)]

45. Wang, Y.; Cheng, M.; Yan, X.; Zhao, P.; Wang, K.; Wang, Y.; Wang, X.; Wang, J. Preparation and characterization of an active packaging film loaded with tea tree oil-hydroxyapatite porous microspheres. *Ind. Crops Prod.* **2023**, *199*, 116783. [[CrossRef](#)]
46. Aziz, S.G.-G.; Almasi, H. Physical characteristics, release properties, and antioxidant and antimicrobial activities of whey protein isolate films incorporated with thyme (*Thymus vulgaris* L.) extract-loaded nanoliposomes. *Food Bioprocess Technol.* **2018**, *11*, 1552–1565. [[CrossRef](#)]
47. Gomide, R.A.C.; de Oliveira, A.C.S.; Luvizaro, L.B.; Yoshida, M.I.; de Oliveira, C.R.; Borges, S.V. Biopolymeric films based on whey protein isolate/lignin microparticles for waste recovery. *J. Food Process Eng.* **2021**, *44*, e13596. [[CrossRef](#)]
48. Amjadi, S.A.; Almasi, H.; Ghadertaj, A.; Mehryar, L. Whey protein isolate-based films incorporated with nanoemulsions of orange peel (*Citrus sinensis*) essential oil: Preparation and characterization. *J. Food Process. Preserv.* **2021**, *45*, e15196. [[CrossRef](#)]

Disclaimer/Publisher’s Note: The statements, opinions and data contained in all publications are solely those of the individual author(s) and contributor(s) and not of MDPI and/or the editor(s). MDPI and/or the editor(s) disclaim responsibility for any injury to people or property resulting from any ideas, methods, instructions or products referred to in the content.